Morphology of nanoscale structures on fused silica surfaces from interaction with temporally tailored femtosecond pulses

Lars Englert, Matthias Wollenhaupt, Cristian Sarpe, Dirk Otto, and Thomas Baumert[a)]
Institut fuer Physik and CINSaT, Universitaet Kassel, Heinrich-Plett-Str. 40, D-34132 Kassel, Germany

(Received 6 October 2011; accepted for publication 2 February 2012; published 16 July 2012)

Laser control of two basic ionization processes on fused silica, i.e., multiphoton ionization and avalanche ionization, with temporally asymmetric pulse envelopes is investigated. Control leads to different final electron densities/energies as the direct temporal intensity profile and the time inverted intensity profile address the two ionization processes in a different fashion. This results in observed different thresholds for material modification on the surface as well as in reproducible lateral structures being an order of magnitude below the diffraction limit (down and below 100 nm at a numerical aperture of 0.5). In this contribution, the morphology of the resulting structures is discussed. © *2012 Laser Institute of America*.

Key words: laser materials processing, laser-induced breakdown, multiphoton processes, nanostructure fabrication, pulse shaping, femtosecond phenomena, ultrafast processes in condensed matter

I. INTRODUCTION

Primary processes induced by ultrafast laser radiation involve nonlinear electronic excitation, energy transfer to the lattice, and phase transitions that occur on fast (femtosecond, picosecond) but material dependent time scales. Optimal energy coupling with the help of suitably shaped temporal pulse envelopes gives thus the possibility to guide the material response towards user-designed directions, offering extended flexibility for quality material processing.[1] Regarding wide gap materials, lasers delivering ultrashort pulses have emerged as a promising tool for a variety of applications ranging from precision micromachining on and below the wavelength of light to medical surgery.[2] Within the context of laser control, it is the transient free-electron density in the conduction band of the dielectric that plays a fundamental role in addition to various propagation and relaxation mechanisms. A large number of experiments make use of the threshold of observed damage as experimental evidence for exceeding a certain critical electron density after the laser interaction. These involve pulse duration measurements[3–5] and pulse-train experiments[6] all showing a strong dependence of the damage threshold on pulse duration and on pulse separation. Direct studies of transient electron densities range from intensities below[7,8] up to well above the breakdown threshold.[9,10] The temporal evolution of the free-electron density and the role of the fundamental ionization processes are strongly depending on time and intensity,[11,12] and a dependence on the instantaneous frequency was also reported.[13] Two main processes for generating free electrons are multiphoton ionization (MPI) and avalanche ionization (AI). MPI requires no free initial free electrons and has highest efficiency for shortest pulses. AI on the other hand needs initial free electrons and needs time to establish. In our work, we make use of temporally asymmetric femtosecond pulses in order to control MPI and AI. Control leads to different final electron densities (and energies) as the direct temporal profile and the time inverted profile address the two ionization processes in a different fashion. This results in observed different thresholds for material modification in fused silica as well as in reproducible lateral structures being an order of magnitude below the diffraction limit. Our original experiments using third order dispersion (TOD) are published in Refs. 14 and 15. Analytic expressions for pulse shapes relevant to material processing are compiled in Refs. 16 and 17. In the latter publication, it was found that a temporally asymmetric pulse envelope based on TOD and its time reversed counterpart—both having constant instantaneous frequency—shows a different threshold for surface material processing, whereas no pronounced differences between up- and down-chirped radiation based on group delay dispersion (GDD) (i.e., symmetric temporal pulse envelope but asymmetric instantaneous frequency) were observed in the measured structure diameters and thresholds. After a short description of the experiment and a short summary of the work performed so far, we present here the morphology of the structures based on scanning electron microscopy (SEM) and atomic force microscopy (AFM).

II. EXPERIMENT

In our experiment, we combine femtosecond pulse shaping techniques[18] (that can reach nowadays zeptosecond precision)[19] with a microscope setup for material processing.[14,20] Linear polarized laser pulses with 35 fs full width at half maximum (FWHM) pulse duration and a central wavelength of 790 nm are provided by an amplified Ti:Sapphire laser system. After passing a calibrated home built spectral phase modulator,[21] the pulses are focused via a Zeiss LD Epiplan 50×0.5 numerical aperture (NA) objective to a spot diameter of 1.4 μm ($1/e^2$ value of intensity profile). The dispersion of

a)Electronic mail: baumert@physik.uni-kassel.de

the objective was measured to be -900 ± 50 fs^2 (GDD) and compensated prior to the experiments. The pulse shaper is properly operated in a parameter regime far away from space time coupling effects[22] as verified also via quantum optical measurements with the same setup.[23,24] Shaped pulses are characterized in the interaction region via second order cross correlation. The sample is translated by a 3-axis piezo table to a new position for each shot. A typical measurement pattern consists of an array of points where we vary the pulse shapes, energy, and focal z-position. After laser processing, the samples are analyzed via SEM and AFM.

III. RESULTS AND DISCUSSION

The results obtained from our earlier experiments[14,15] are summarized in Fig. 1. Systematic studies with phase shaped laser pulses based on TOD leading to asymmetric temporally shaped laser pulses revealed a change in the threshold depending on whether the direct pulse shape or the time inverted profile was used [see Fig. 1(A)]. Theoretical simulations based on a multiple rate equation (MRE) model described in Ref. 12 show that it is the timing of an intense photoionizing subpulse which can turn on or off AI. The observed nanoscale structures are an order of magnitude below the diffraction limit and remarkably stable with respect to variations in laser fluence [see Fig. 1(C)]. Applying pure second order dispersion at threshold, also subdiffraction structures are created; however, no substructure being stable with respect to laser fluence variations was observed.[17]

In Fig. 2, the observed morphologies for bandwidth limited pulses and TOD shaped pulses are summarized. Our original data were analyzed mainly via SEM. Recently, we turned to AFM characterization in addition. A systematic comparison between AFM and SEM structures obtained with bandwidth limited pulses (not shown) revealed that for the outer structure AFM and SEM, measurements gave the same diameters, whereas for the inner diameter, the SEM structures are about 10% smaller as compared to structures determined via AFM. We define the inner diameter determined by AFM by the diameter at which the height profile falls below the unperturbed surface level [see Fig. 2(B)]. The maximum depth of the generated structures may be limited by the shape of the used high aspect ratio tip. The shape of the high aspect ratio tip is also responsible for the asymmetry in profile seen in Fig. 2(B). At threshold, the structures are a few 10 nm in depth.

The intriguing observation in Fig. 2 is that the observed substructure for unshaped pulses occurs only for high intensities and is embedded in a large area defined by the inner structure, whereas for the TOD shaped pulses, this substructure starts to appear already at threshold. On a first glance, the substructure might be attributed to filamentation processes as observed in bulk fused silica under similar excitation conditions[25] as well as on surfaces of dielectrics[26,27] and reviewed in Ref. 28. However, as filamentation usually needs propagation to occur, the lack of observed propagation structures especially for the TOD shaped pulses may rule out filamentation as the only explanation. Note that no plasma in air was observed at the applied laser energies.

In order to investigate to what extent the seed and heat model explaining the differences in observed ablation threshold for temporally asymmetric pulse shapes may be extended

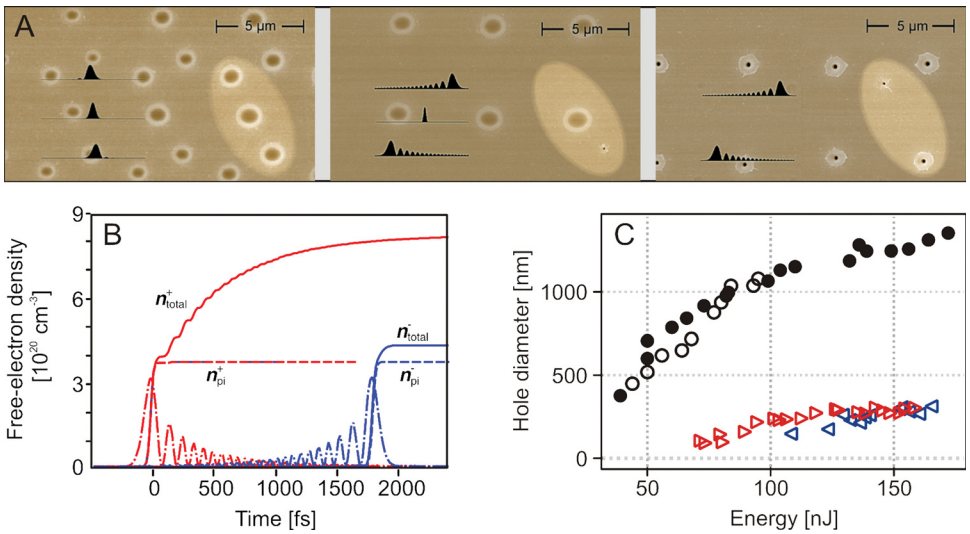

FIG. 1. (A) SEM micrographs of a measurement pattern on fused silica: For an applied energy E and focal position, a triplet of applied laser pulses is highlighted by the ellipse. Negative, zero, and positive TODs were used where the corresponding normalized temporal intensity profiles are sketched in black for different TODs. Left: low TOD (TOD $= \pm 2.5 \times 10^4$ fs^3, statistic pulse duration of $2\sigma = 50$ fs, $E = 77$ nJ) results in negligible differences between created structures. Middle: high positive TOD (TOD $= +6 \times 10^5$ fs^3, statistic pulse duration of $2\sigma = 960$ fs, $E = 71$ nJ) results in a change of structure size and threshold energy. Right: the threshold energy for ablation with high negative TOD (-6×10^5 fs^3) is reached with $E = 110$ nJ. Here, the unshaped pulse is suppressed in order not to mask structures with TOD. (B) Transient free-electron density n_{total} (solid lines) as calculated with help of the MRE, together with the density of electrons provided by photoionization n_{pi} (dashed lines), and the corresponding transient intensities (dashed-dotted lines) of the pulse with positive TOD (index +) and negative TOD (index −), respectively. (C) Inner diameters (see Fig. 2) of ablation structures as a function of pulse energy for unshaped pulses (circles). For (+) shaped pulses (triangles pointing right) and for (−) shaped pulses (triangles pointing left), the diameter of the substructure is displayed. Without changing the focus spot diameter, substructures below 300 nm are obtained over a large energy range, thus providing a large process window for creation of nanostructures. The smallest structures are about 100 nm in diameter.

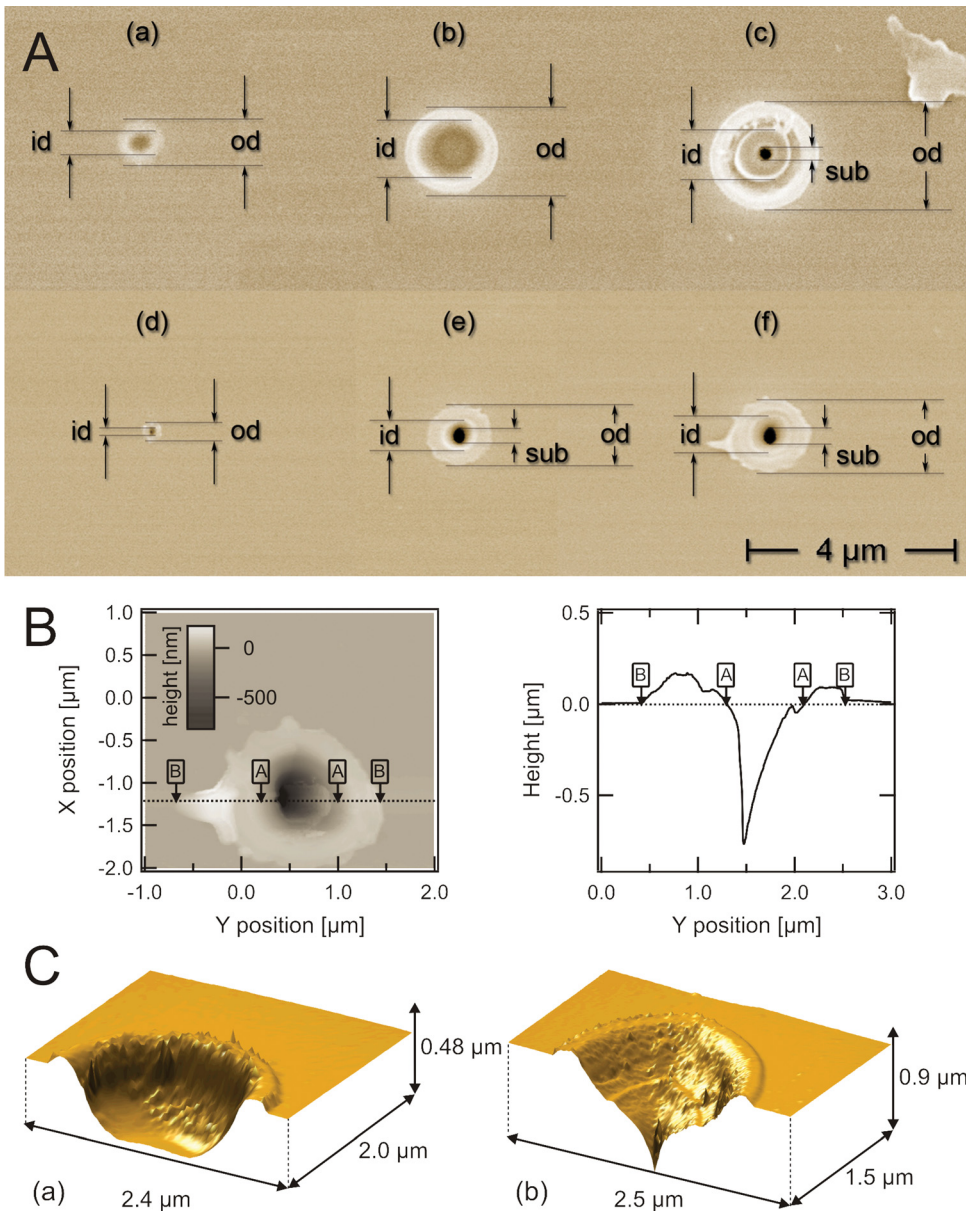

FIG. 2. (A) SEM micrographs for selected structures of Fig. 1(C). *od* = outer diameter, *id* = inner diameter, and sub = diameter of substructure. For unshaped pulses at threshold for material processing (40 nJ) (a), at intermediate energy (140 nJ) (b), and at high energy (240 nJ) (c). Structures for high positive TOD (TOD = $+6 \times 10^5$ fs^3) at threshold (d), at intermediate energy (120 nJ) (e), and at high energy (150 nJ) (f). At threshold, the substructure merges into the inner structure. For unshaped pulses, the substructure occurs only for high intensities and is embedded in a large area defined by the inner structure. (B) AFM image of structure Af. The distance BB defines the outer diameter *od* and AA defines the inner diameter *id*. Note the high aspect ratio of the 800 nm deep structure. As a general trend, the depth of the structures increased approximately linearly from the threshold up to 50 nJ above threshold in a range from several 10 to several 100 nm for positive and negative phase masks. (C). Typical AFM structures for the unshaped laser pulse. In the energy range up to 140 nJ, a shallow crater is observed (a), whereas in the energy range from 150 to 250 nJ, the additional small substructure appears (b).

to explain the spatial observations, we started simulations. The motivation stems from the simple picture that an initial part of the pulse structure may create free electrons in a spatially very confined region well below the damage threshold via MPI and the remaining pulse exploits AI to reach the critical energy also in a very restricted area. In that simulations, we solve rate equations for a Gaussian spatial beam profile taking MPI, AI, and recombination into account as a function of various temporal profiles. So far we did not get a conclusive picture from these simulations: in the calculations, the threshold of material ablation was set by reaching a certain electron density. This criterion allowed to describe the threshold for material ablation correctly for various temporal profiles obtained by combining short pulses with long pulses (an example is given in Fig. 3); however, the structure diameter (inner structure) as a function of fluence was sometimes over estimated and sometimes under estimated compared to the measured ones. The substructure behavior was never reproduced in this approach. Currently, we speculate, in addition, to what extent nanoplasmonic effects like, for example, near field effects from a spatially confined region of high electron densities created by a part of the temporal structured laser pulse can also be responsible for part of the observations.

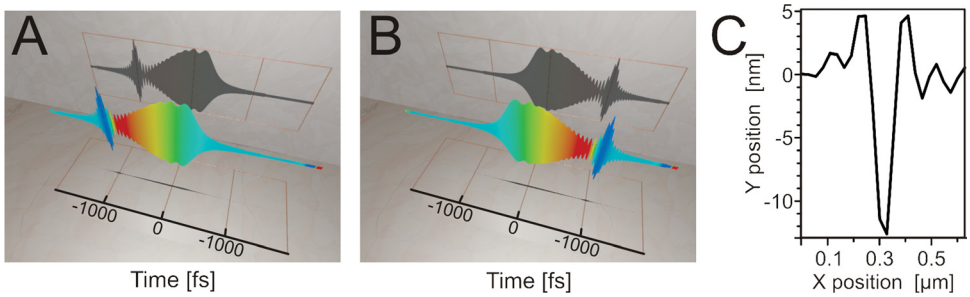

FIG. 3. Nanoscale structures by pulse shapes combining pulses stretched via GGD with a short pulse. (A) A short pulse followed by an up-chirp is generated by a spectral phase function consisting of a linear phase $\varphi(\omega)=\phi_1\cdot(\omega-\omega_0)$ for the blue part of the spectrum ($\lambda<782$ nm) and a quadratic spectral phase $\varphi(\omega)=\phi_2\cdot(\omega-\omega_0)^2$ for the red part of the spectrum ($\lambda>782$ nm), where $\phi_1=-1000$ fs and $\phi_2=1000$ fs^2. (B) Time inversion of the pulse shape by setting $\phi_1=1000$ fs and $\phi_2=-1000$ fs^2 produces a down-chirped pulse followed by a short pulse. (C) We obtain structures slightly below 100 nm as shown in the AFM trace for pulses shown in (B). The threshold energy in this case is about 90 nJ.

In order to test the seed and heat hypothesis further, we experimentally also used pulse shapes combining pulses stretched via GGD with a short pulse. At threshold, we again obtain structures with a diameter slightly below 100 nm (see Fig. 3). Dedicated double pulse experiments up to 10 ps with the help of our latest pulse shaping setup[19] are currently performed in our labs in addition in order to study early stage material modifications. An extension of the experiments to materials with different orders of the MPI process seems to be a promising route for a better understanding as well.

IV. CONCLUSIONS

We conclude that control of ionization processes with tailored femtosecond pulses is an important—although not complete—prerequisite for robust control of laser processing of high band gap materials on the nanometer scale. We gave evidence that our strategy opens the route to develop tailored pulse shapes for controlled nanoscale material processing of dielectrics.

ACKNOWLEDGMENT

The financial support of DFG via the priority program SPP 1327 is gratefully acknowledged.

[1]R. Stoian, M. Wollenhaupt, T. Baumert, and I. V. Hertel, *Laser Precision Microfabrication*, edited by K. Sugioka, M. Meunier, and A. Piqué (Springer-Verlag, Berlin, 2010), pp. 121–144.
[2]A. Vogel, J. Noack, G. Hüttman, and G. Paltauf, "Mechanism of femtosecond laser nanosurgery of cells and tissues," Appl. Phys. B **81**, 1015–1047 (2005).
[3]B. C. Stuart, M. D. Feit, A. M. Rubenchik, B. W. Shore, and M. D. Perry, "Laser-induced damage in dielectrics with nanosecond to subpicosecond pulses," Phys. Rev. Lett. **74**, 2248–2251 (1995).
[4]A. C. Tien, S. Backus, H. C. Kapteyn, M. M. Murnane, and G. Mourou, "Short-pulse laser damage in transparent materials as a function of pulse duration," Phys. Rev. Lett. **82**, 3883–3886 (1999).
[5]M. Lenzner, J. Krüger, S. Sartania, Z. Cheng, Ch. Spielmann, G. Mourou, W. Kautek, and F. Krausz, "Femtosecond optical breakdown in dielectrics," Phys. Rev. Lett. **80**, 4076–4079 (1998).
[6]R. Stoian, M. Boyle, A. Thoss, A. Rosenfeld, G. Korn, and I. V. Hertel, "Dynamic temporal pulse shaping in advanced ultrafast laser material processing," Appl. Phys. A **77**, 265–269 (2003).
[7]S. S. Mao, F. Quéré, S. Guizard, X. Mao, R. E. Russo, G. Petite, and P. Martin, "Dynamics of femtosecond laser interactions with dielectrics," Appl. Phys. A **79**, 1695–1709 (2004).
[8]V. V. Temnov, K. Sokolowski-Tinten, P. Zhou, A. El-Khamhawy, and D. von der Linde, "Multiphoton ionization in dielectrics: Comparison of circular and linear polarization," Phys. Rev. Lett. **97**, 237403-1–237403-4 (2006).
[9]I. H. Chowdhury, X. Xu, and A. M. Weiner, "Ultrafast double-pulse ablation of fused silica," Appl. Phys. Lett. **86**, 151110-1–151110-3 (2005).
[10]C. Sarpe-Tudoran, A. Assion, M. Wollenhaupt, M. Winter, and T. Baumert, "Plasma dynamics of water breakdown at a water surface induced by femtosecond laser pulses," Appl. Phys. Lett. **88**, 261109-1–261109-3 (2006).
[11]A. Kaiser, B. Rethfeld, M. Vicanek, and G. Simon, "Microscopic processes in dielectrics under irradiation by subpicosecond laser pulses," Phys. Rev. B **61**, 11437–11450 (2000).
[12]B. Rethfeld, "Unified model for the free-electron avalanche in laser-irradiated dielectrics," Phys. Rev. Lett. **92**, 187401-1–187401-4 (2004).
[13]E. Louzon, Z. Henis, S. Pecker, Y. Ehrlich, D. Fisher, M. Fraenkel, and A. Zigler, "Reduction of damage threshold in dielectric materials induced by negatively chirped laser pulses," Appl. Phys. Lett. **87**, 241903-1–241903-3 (2005).
[14]L. Englert, B. Rethfeld, L. Haag, M. Wollenhaupt, C. Sarpe-Tudoran, and T. Baumert, "Control of ionization processes in high band gap materials via tailored femtosecond pulses," Opt. Express **15**, 17855–17862 (2007).
[15]L. Englert, M. Wollenhaupt, L. Haag, C. Sarpe-Tudoran, B. Rethfeld, and T. Baumert, "Material processing of dielectrics with temporally asymmetric shaped femtosecond laser pulses on the nanometer scale," Appl. Phys. A **92**, 749–753 (2008).
[16]M. Wollenhaupt, L. Englert, A. Horn, and T. Baumert, "Control of ionization processes in high band gap materials," J. Laser Micro/Nanoeng. **4**, 144–151 (2009).
[17]M. Wollenhaupt, L. Englert, A. Horn, and T. Baumert, "Temporal femtosecond pulse tailoring for nanoscale laser processing of wide-bandgap materials," in *Proceedings of SPIE, Ultrafast Phenomena in Semiconductors and Nanostructures Materials XIV*, edited by J.-J. Song, K.-T. Tsen, M. Betz, A. Y. Elezzabi, (SPIE, 2010), Vol. 7600, pp. 76000X-1–76000X-11.
[18]A. M. Weiner, "Femtosecond pulse shaping using spatial light modulators," Rev. Sci. Instrum. **71**, 1929–1960 (2000).
[19]J. Köhler, M. Wollenhaupt, T. Bayer, C. Sarpe, and T. Baumert, "Zeptosecond precision pulse shaping," Opt. Express **19**, 11638–11653 (2011).
[20]A. Assion, M. Wollenhaupt, L. Haag, F. Mayorov, C. Sarpe-Tudoran, M. Winter, U. Kutschera, and T. Baumert, "Femtosecond laser-induced breakdown spectrometry for Ca^{2+} analysis of biological samples with high spatial resolution," Appl. Phys. B **77**, 391–397 (2003).
[21]A. Präkelt, M. Wollenhaupt, A. Assion, C. Horn, C. Sarpe-Tudoran, M. Winter, and T. Baumert, "Compact, robust and flexible setup for femtosecond pulse shaping," Rev. Sci. Instrum. **74**, 4950–4953 (2003).
[22]B. J. Sussman, R. Lautsen, and A. Stolow, "Focusing of light following a 4-f pulse shaper: Considerations for quantum control," Phys. Rev. A **77**, 043416-1–043416-11 (2008).
[23]T. Bayer, M. Wollenhaupt, and T. Baumert, "Strong-field control landscapes of coherent electronic excitation," J. Phys. B **41**, 074007-1–074007-13 (2008).
[24]T. Bayer, M. Wollenhaupt, C. Sarpe-Tudoran, and T. Baumert, "Robust photon locking," Phys. Rev. Lett. **102**, 023004-1–023004-4 (2009).

[25]A. Couairon, L. Sudrie, M. Franco, B. Prade, and A. Mysyrowicz, "Filamentation and damage in fused silica induced by tightly focused femtosecond laser pulses," Phys. Rev. B **71**, 125435-1–125435-11 (2005).
[26]Y. V. White, X. Li, Z. Sikorski, L. M. Davis, and W. Hofmeister, "Single-pulse ultrafast-laser machining of high aspect nano-holes at the surface of SiO2," Opt. Express **16**, 14411–14420 (2008).
[27]B. Delobelle, F. Courvoisier, and P. Delobelle, "Morphology study of femtosecond laser nano-structured borosilicate glass using atomic force microscopy and scanning electron microscopy," Opt. Lasers Eng. **48**, 616–625 (2009).
[28]A. Couairon and A. Mysyrowicz, "Femtosecond filamentation in transparent media," Phys. Rep. **441**, 47–189 (2007).